

# UC Davis

## UC Davis Previously Published Works

### Title

Impaired BK<sub>Ca</sub> channel function in native vascular smooth muscle from humans with type 2 diabetes.

### Permalink

<https://escholarship.org/uc/item/03r5k91k>

### Journal

Scientific reports, 7(1)

### ISSN

2045-2322

### Authors

Nieves-Cintrón, Madeline  
Syed, Arsalan U  
Buonarati, Olivia R  
et al.

### Publication Date

2017-10-01

### DOI


10.1038/s41598-017-14565-9

Peer reviewed

# SCIENTIFIC REPORTS

OPEN

## Impaired BK<sub>Ca</sub> channel function in native vascular smooth muscle from humans with type 2 diabetes

Madeline Nieves-Cintrón<sup>1</sup>, Arsalan U. Syed<sup>1</sup>, Olivia R. Buonarati<sup>1</sup>, Robert R. Rigor<sup>1</sup>, Matthew A. Nystoriak<sup>2</sup>, Debapriya Ghosh<sup>1</sup>, Kent C. Sasse<sup>3</sup>, Sean M. Ward<sup>4</sup>, Luis F. Santana<sup>5</sup>, Johannes W. Hell<sup>1</sup> & Manuel F. Navedo<sup>1</sup> 

Large-conductance Ca<sup>2+</sup>-activated potassium (BK<sub>Ca</sub>) channels are key determinants of vascular smooth muscle excitability. Impaired BK<sub>Ca</sub> channel function through remodeling of BK<sub>Ca</sub>  $\beta$ 1 expression and function contributes to vascular complications in animal models of diabetes. Yet, whether similar alterations occur in native vascular smooth muscle from humans with type 2 diabetes is unclear. In this study, we evaluated BK<sub>Ca</sub> function in vascular smooth muscle from small resistance adipose arteries of non-diabetic and clinically diagnosed type 2 diabetic patients. We found that BK<sub>Ca</sub> channel activity opposes pressure-induced constriction in human small resistance adipose arteries, and this is compromised in arteries from diabetic patients. Consistent with impairment of BK<sub>Ca</sub> channel function, the amplitude and frequency of spontaneous BK<sub>Ca</sub> currents, but not Ca<sup>2+</sup> sparks were lower in cells from diabetic patients. BK<sub>Ca</sub> channels in diabetic cells exhibited reduced Ca<sup>2+</sup> sensitivity, single-channel open probability and tamoxifen sensitivity. These effects were associated with decreased functional coupling between BK<sub>Ca</sub>  $\alpha$  and  $\beta$ 1 subunits, but no change in total protein abundance. Overall, results suggest impairment in BK<sub>Ca</sub> channel function in vascular smooth muscle from diabetic patients through unique mechanisms, which may contribute to vascular complications in humans with type 2 diabetes.

The World Health Organization estimates that ~350 million people worldwide have non-insulin-dependent type 2 diabetes, a number that is expected to double by 2030<sup>1</sup>. Vascular complications (e.g. hypertension, coronary heart disease, stroke) are among the most prominent causes of morbidity and mortality in type 2 diabetic patients<sup>1–3</sup>. While endothelial dysfunction has long been recognized as a key link in the pathogenesis of vascular complications during diabetes, emerging data in human and animal models also implicate vascular smooth muscle dysfunction in this process<sup>3–11</sup>. At present however, there is limited information about the mechanisms underlying changes in vascular smooth muscle function in native cells from type 2 diabetic patients.

The contractile state of vascular smooth muscle in small resistance arteries is controlled by multiple ion channels<sup>12</sup>. Among them, large-conductance Ca<sup>2+</sup>-activated potassium (BK<sub>Ca</sub>) channels play a key role in control of vascular smooth muscle contractility via tonic regulation of membrane potential<sup>13</sup>. Physiologically, these channels are activated by membrane depolarization and localized Ca<sup>2+</sup> release events through ryanodine receptors (e.g. Ca<sup>2+</sup> sparks) located in the sarcoplasmic reticulum<sup>13–15</sup>. The opening of BK<sub>Ca</sub> channels by Ca<sup>2+</sup> sparks results in the occurrence of BK<sub>Ca</sub>-mediated spontaneous transient outward currents (STOCs), leading to vascular smooth muscle hyperpolarization and consequently vasodilation. Conversely, their inhibition causes membrane potential depolarization and vasoconstriction. BK<sub>Ca</sub> channels are composed of four pore-forming  $\alpha$  subunits in association with accessory  $\beta$  subunits<sup>16</sup>. Four distinct BK<sub>Ca</sub>  $\beta$  subunits ( $\beta$ 1– $\beta$ 4) have been identified, with BK<sub>Ca</sub>  $\beta$ 1 being predominantly expressed in vascular smooth muscle<sup>16</sup>. The BK<sub>Ca</sub>  $\beta$ 1 subunit regulates BK<sub>Ca</sub> channel activity by modulating its apparent Ca<sup>2+</sup> sensitivity as well as its biophysical properties<sup>17</sup>. Impairment in BK<sub>Ca</sub>  $\beta$ 1 expression and function has been implicated in aberrant vascular BK<sub>Ca</sub> channel activity in animal models of diabetes and hypertension, and in immortalized cell lines from human diabetic subjects<sup>9,18–25</sup>. However, whether similar

<sup>1</sup>Department of Pharmacology, University of California, Davis, CA, 95616, USA. <sup>2</sup>Diabetes and Obesity Center, Department of Medicine, University of Louisville, Louisville, KY, 40202, USA. <sup>3</sup>Sasse Surgical Associates, Reno, NV, 89502, USA. <sup>4</sup>Department of Physiology and Cell Biology, University of Nevada, Reno School of Medicine, Reno, NV, 89557, USA. <sup>5</sup>Department of Physiology & Membrane Biology, University of California, Davis, CA, 95616, USA. Correspondence and requests for materials should be addressed to M.N.-C. (email: [mcnieves@ucdavis.edu](mailto:mcnieves@ucdavis.edu)) or M.F.N. (email: [mfnavedo@ucdavis.edu](mailto:mfnavedo@ucdavis.edu))

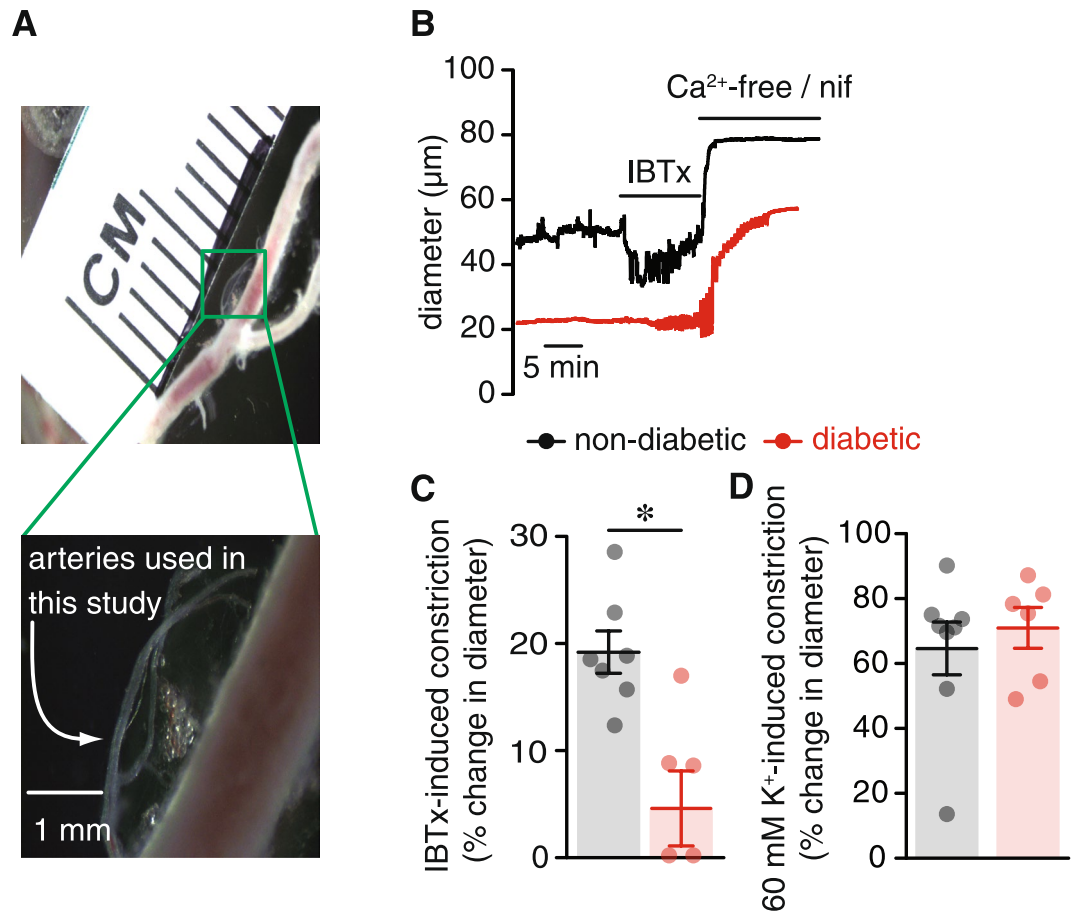


**Figure 1.** Adipose arteries from diabetic subjects exhibit blunted response to IBTx. **(A)** Exemplary image of small resistance adipose arteries used in this study. The image below shows an expanded view of the area in the green square. **(B)** Representative diameter recordings of pressurized (80 mmHg) adipose arteries from non-diabetic and diabetic patients before and after perfusion of 100 nM iberiotoxin or a  $\text{Ca}^{2+}$  free + nifedipine (1  $\mu\text{M}$ ) solution. **(C)** Summary of iberiotoxin-induced constriction in non-diabetic ( $n = 7$  arteries, 4 subjects) and diabetic ( $n = 5$  arteries, 5 subjects) adipose arteries pressurized to 80 mmHg. **(D)** Scatter/bar plot summarizing vascular tone at 80 mmHg in response to 60 mM extracellular  $\text{K}^+$  in non-diabetic ( $n = 8$  arteries, 4 subjects) and diabetic ( $n = 6$  arteries, 5 subjects) adipose arteries.  $*P < 0.05$ , Mann-Whitney test. Significance was compared between non-diabetic and diabetic datasets.

alterations in  $\text{BK}_{\text{Ca}}$  channel activity occur in native, freshly dissociated vascular smooth muscle cells from humans with type 2 diabetes has not been established.

Here, we investigated  $\text{BK}_{\text{Ca}}$  channel function in freshly isolated, small resistance adipose arteries and corresponding native vascular smooth muscle cells from obese non-diabetic and clinically diagnosed type 2 diabetic patients. Data revealed a reduction in iberiotoxin (IBTx) sensitivity of intact arteries from diabetic patients. This was associated with impaired  $\text{BK}_{\text{Ca}}$  channel activity due to decreased  $\text{BK}_{\text{Ca}}$   $\beta 1$  function in diabetic vascular smooth muscle cells. In contrast to results observed in animal models<sup>9,21–23,25</sup>, impaired  $\text{BK}_{\text{Ca}}$   $\beta 1$  function was not due to changes in  $\text{BK}_{\text{Ca}}$   $\beta 1$  abundance, but to a reduced functional association between  $\text{BK}_{\text{Ca}}$   $\alpha$  and  $\beta 1$  subunits in diabetic cells. Thus, results suggest a mechanism for altered vascular  $\text{BK}_{\text{Ca}}$  channel function in patients with type 2 diabetes with similar, but not identical features to those observed in animal models of diabetes.

## Results

To establish whether  $\text{BK}_{\text{Ca}}$  channel function is impaired in native vascular smooth muscle cells during type 2 diabetes, small diameter arteries were dissected from adipose tissue obtained from obese non-diabetic and clinically diagnosed type 2 diabetic patients undergoing surgical sleeve gastrectomy (see Methods section). Available patient information is included in Supplementary Table S1.

**Decreased IBTx sensitivity in arteries from diabetic subjects.** Small diameter adipose arteries (average passive diameter between 50–90  $\mu\text{m}$ ; see Fig. 1A) from non-diabetic and clinically diagnosed diabetic patients were pressurized to 80 mmHg, and allowed to develop stable myogenic tone. Mean basal myogenic tone was  $44 \pm 9\%$  in non-diabetic arteries, and was modestly, although not significantly, elevated to  $49 \pm 3\%$  in arteries from diabetic patients ( $P = 0.325$ ). To assess the contribution of  $\text{BK}_{\text{Ca}}$  channels to vascular function, adipose arteries from non-diabetic and diabetic patients were challenged with the selective  $\text{BK}_{\text{Ca}}$  channel inhibitor iberiotoxin

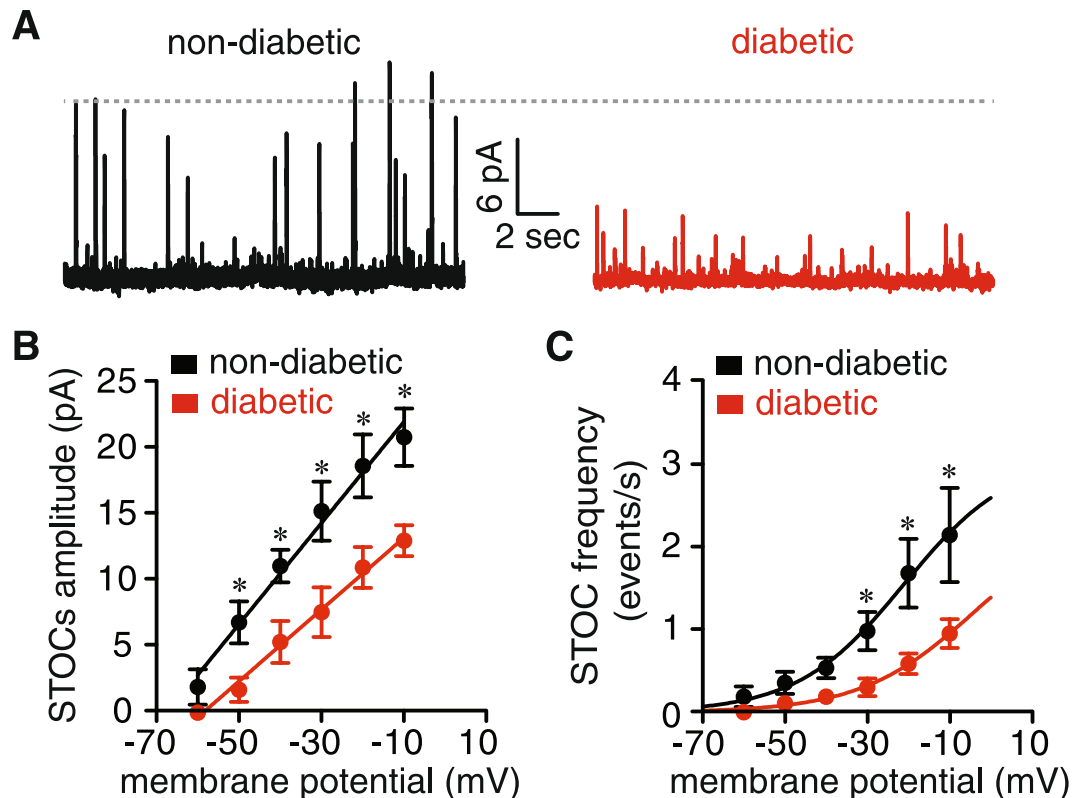


**Figure 2.** STOCs amplitude and frequency are reduced in vascular smooth muscle from diabetic patients. (A) Representative traces of spontaneous whole-cell  $BK_{Ca}$  currents (e.g. STOCs) at  $-40$  mV in vascular smooth muscle from non-diabetic and diabetic patients. (B,C) Voltage dependency of STOC amplitude (B) and frequency (C) in cells from non-diabetic ( $n = 10$  cells, 4 subjects) and diabetic ( $n = 13$  cells, 4 subjects) patients. Solid lines represent the best fit of the amplitude data using a linear regression function and of the frequency data using a Boltzmann sigmoidal function.  $*P < 0.05$ , unpaired  $t$  test. Significance was compared between corresponding non-diabetic and diabetic datasets.

(IBTx; 100 nM). IBTx caused robust vasoconstriction in non-diabetic arteries (24% decrease in diameter) (Fig. 1B and C; Supplementary Table S2). This is consistent with  $BK_{Ca}$  channel activity opposing vasoconstriction. In contrast, IBTx had little effect on pressurized adipose arteries from diabetic patients (4% decrease in diameter; Fig. 1B and C; Supplementary Table S2;  $P < 0.05$ ). Arteries from both groups responded to external application of a 60 mM  $K^+$  solution with robust constriction (Fig. 1D; Supplementary Table S2), suggesting that differences in the IBTx response were not simply due to the inability of diabetic arteries to respond to a contractile stimulus. This decrease in IBTx sensitivity in diabetic arteries suggests impairment in  $BK_{Ca}$  channel function in arteries from diabetic patients.

**Decreased STOC amplitude and frequency in vascular smooth muscle from diabetic patients.**  $BK_{Ca}$ -mediated STOCs were recorded at membrane potential ranging from  $-60$  mV to  $-10$  mV. Figure 2A displays representative STOCs recordings from freshly dissociated vascular smooth muscle obtained from small diameter adipose arteries from non-diabetic and diabetic patients at  $-40$  mV. STOCs amplitude and frequency increased with membrane depolarization in cells of both groups. However, a significant reduction in STOC amplitude was evident at several membrane potentials examined in cells from diabetic compared to non-diabetic patients (Fig. 2A and B). The slope of the STOC amplitude-voltage relationship was significantly smaller in diabetic ( $0.27 \pm 0.01$  pA/mV) compared to non-diabetic cells ( $0.38 \pm 0.02$  pA/mV;  $P < 0.05$ ;  $F$  test) (Fig. 1B). STOC frequency was also significantly decreased in diabetic vascular smooth muscle cells at voltages from  $-30$  to  $-10$  mV (Fig. 1C;  $P < 0.05$ ). The voltage dependency of STOC frequency was shifted toward more depolarized potentials in diabetic cells ( $V_{50} = -4 \pm 4$  mV) compared to non-diabetic cells ( $V_{50} = -21 \pm 7$  mV; Fig. 2C). These results suggest that  $BK_{Ca}$  channel activity is altered in vascular smooth muscle from diabetic patients.

**$Ca^{2+}$  spark activity is similar in vascular smooth muscle from non-diabetic and diabetic patients.** STOC activity in vascular smooth muscle is tightly coupled to  $Ca^{2+}$  sparks<sup>13,15,26</sup>. These events were recorded from non-diabetic and diabetic vascular smooth muscle loaded with the fluorescent  $Ca^{2+}$  indicator fluo-4 AM to evaluate whether changes in  $Ca^{2+}$  spark activity could account for impairment in  $BK_{Ca}$  channel function in vascular smooth muscle from diabetic patients (Fig. 3A). Figure 3B and C shows that the amplitude and frequency of  $Ca^{2+}$  sparks were similar in non-diabetic and diabetic cells. These results suggest that impaired

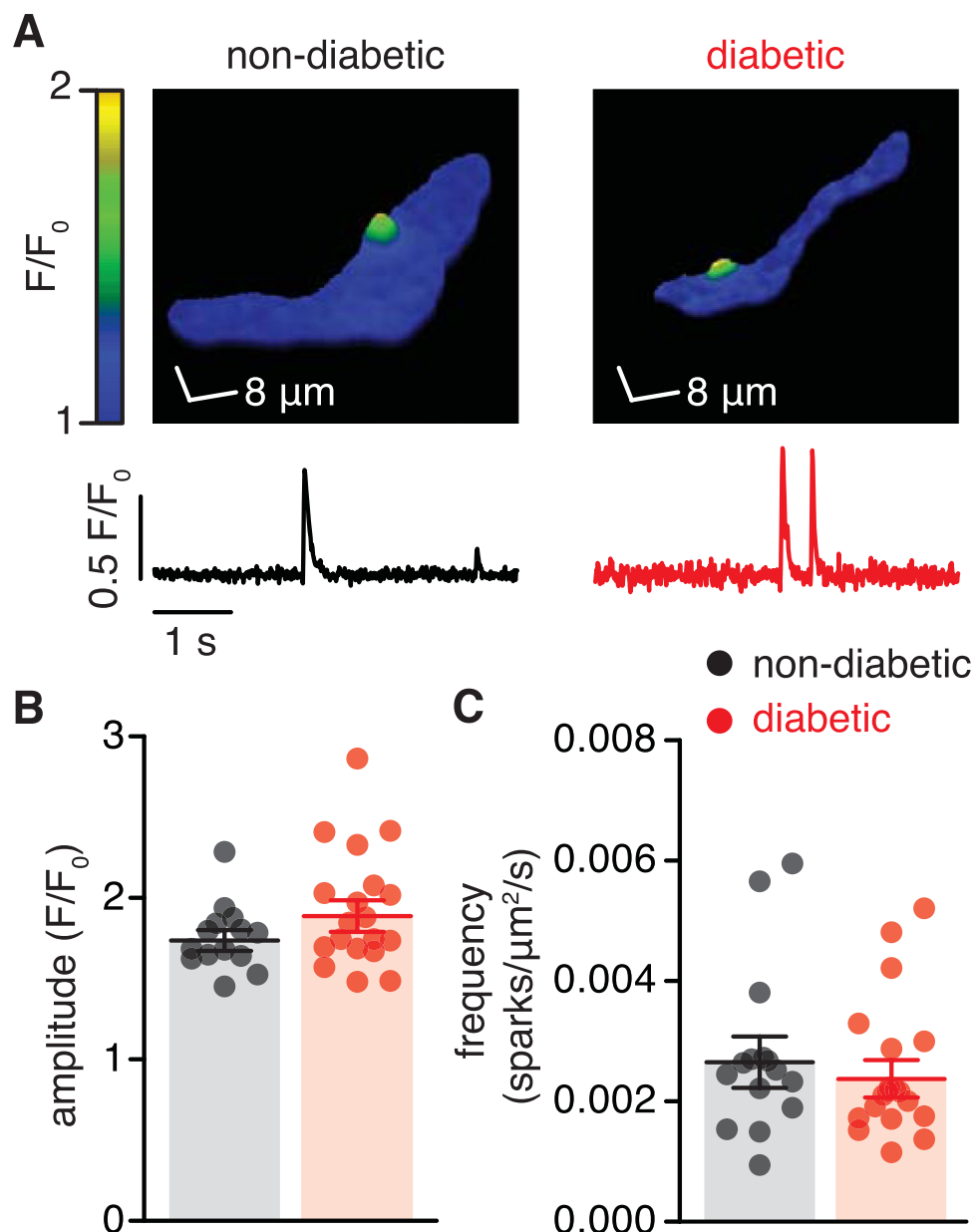


**Figure 3.** The frequency and amplitude of  $\text{Ca}^{2+}$  sparks is similar in non-diabetic and diabetic vascular smooth muscle. (A) Representative three-dimensional pseudo-color images of  $\text{Ca}^{2+}$  sparks (upper panels) and fractional fluorescence traces ( $F/F_0$ ; lower panels) from those sites in fluo-4 AM-loaded vascular smooth muscle cells from non-diabetic and diabetic patients. Scatter/bar plots summarizing  $\text{Ca}^{2+}$  spark amplitude (B) and frequency (C) in cells from non-diabetic ( $n = 254$  events, 14 cells, 3 subjects) and diabetic ( $n = 333$  events, 19 cells, 5 subjects) patients.  $*P < 0.05$ , Mann-Whitney test. Significance was compared between non-diabetic and diabetic datasets.

$\text{BK}_{\text{Ca}}$  channel function is not due to changes in  $\text{Ca}^{2+}$  spark activity in vascular smooth muscle from diabetic patients.

**Impaired  $\text{BK}_{\text{Ca}}$  activity in vascular smooth muscle from diabetic patients.** Single  $\text{BK}_{\text{Ca}}$  currents were recorded in excised membrane patches to evaluate whether differences in the functional properties of  $\text{BK}_{\text{Ca}}$  channels account for compromised channel activity during diabetes.  $\text{BK}_{\text{Ca}}$  currents were monitored at a physiological membrane potential ( $-40$  mV) with bath solution containing either  $1 \mu\text{M}$  or  $10 \mu\text{M}$  free  $\text{Ca}^{2+}$ . Increasing free  $\text{Ca}^{2+}$  from  $1 \mu\text{M}$  to  $10 \mu\text{M}$  augmented the open probability ( $P_o$ ) of  $\text{BK}_{\text{Ca}}$  channels in both non-diabetic and diabetic cells (Fig. 4A and B). However,  $\text{BK}_{\text{Ca}}$  channel  $P_o$  was significantly lower in diabetic cells compared to non-diabetic cells at each  $\text{Ca}^{2+}$  concentration tested (Fig. 4A and B). In addition, open time histograms revealed a shift toward shorter openings in diabetic cells (Fig. 4C;  $P < 0.05$ ;  $F$  test). These results suggest a reduction in apparent  $\text{Ca}^{2+}$  sensitivity and dwell open time of  $\text{BK}_{\text{Ca}}$  channels in vascular smooth muscle cells from diabetic patients.

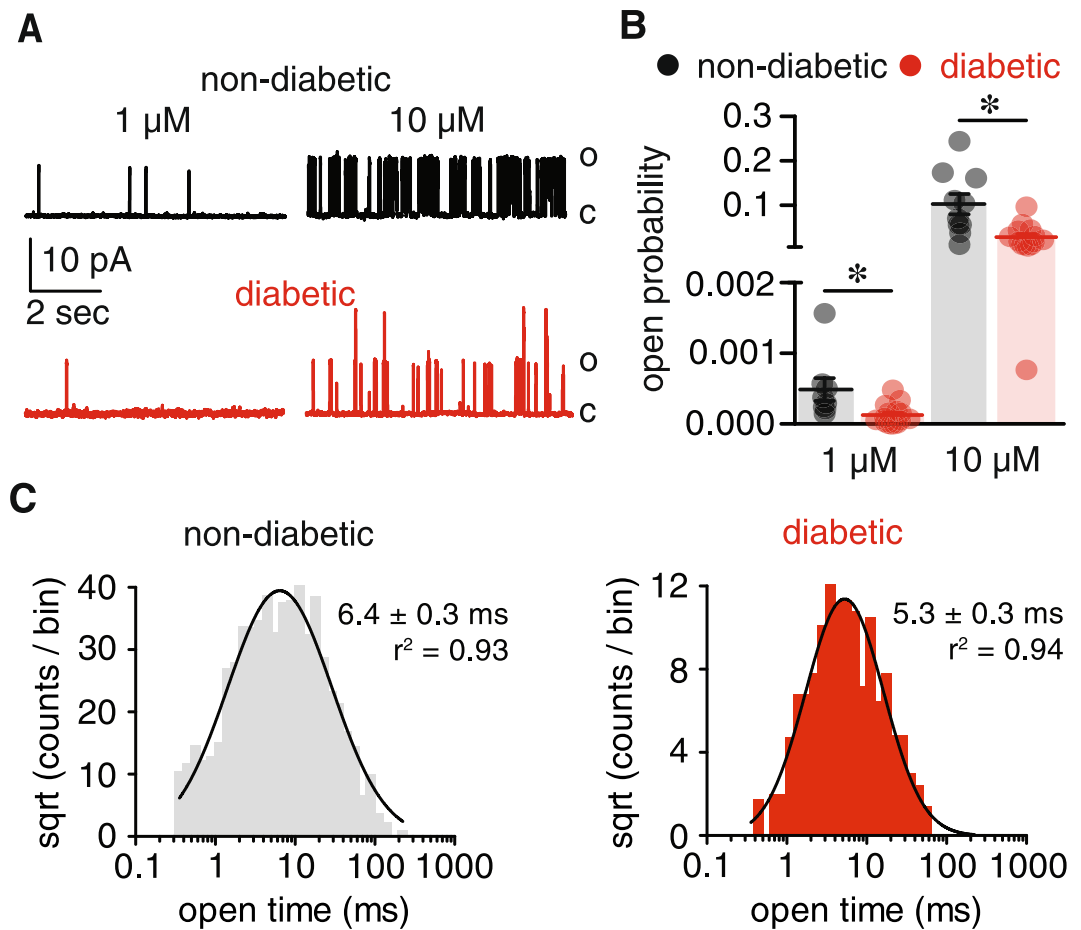


**Figure 4.** Decreased BK<sub>Ca</sub> channel activity in vascular smooth muscle from diabetic patients. (A) Representative single BK<sub>Ca</sub> channel traces at -40 mV from excised membrane patches of isolated human non-diabetic and diabetic vascular smooth muscle cells in the presence of 1 μM and 10 μM free Ca<sup>2+</sup> bath solution (C: closed; O: open). (B) Scatter/bar plot summarizing BK<sub>Ca</sub> channel open probability (P<sub>o</sub>) at the indicated free Ca<sup>2+</sup> concentration from human non-diabetic (n = 18 cells, 9 subjects) and diabetic (n = 27 cells, 15 subjects) cells. \*P < 0.05, Mann-Whitney test. (C) Open dwell time histograms of BK<sub>Ca</sub> channels in non-diabetic and diabetic vascular smooth muscle. The goodness of the fit was assessed with R<sup>2</sup> and the F test was used for comparison between open time fits. Significance was compared between non-diabetic and diabetic datasets.

**Altered BK<sub>Ca</sub> β1 subunit function in vascular smooth muscle from diabetic patients.** The BK<sub>Ca</sub> channel function is highly dependent on expression and function of the accessory BK<sub>Ca</sub> β subunit<sup>17,27</sup>. To examine whether impaired BK<sub>Ca</sub> channel activity in vascular smooth muscle from diabetic patients is due to changes in BK<sub>Ca</sub> β subunit function, single BK<sub>Ca</sub> currents were recorded in the absence or presence of tamoxifen (1 μM). This drug increases BK<sub>Ca</sub> channel P<sub>o</sub> by engaging the BK<sub>Ca</sub> β subunit as shown in Fig. 5A and B, and as previously reported by our group and others<sup>9,19,28</sup>. Whereas tamoxifen significantly increased the P<sub>o</sub> of BK<sub>Ca</sub> in non-diabetic cells, it had a minimal effect in vascular smooth muscle from diabetic subjects (Fig. 5C and D). These results suggest that a reduction in BK<sub>Ca</sub> β subunit function may contribute to impaired BK<sub>Ca</sub> channel activity in vascular smooth muscle cells from diabetic patients.

**Reduced association between BK<sub>Ca</sub> α and BK<sub>Ca</sub> β1 subunits in vascular smooth muscle from diabetic patients.** To examine the molecular mechanisms underlying altered BK<sub>Ca</sub> channel activity and BK<sub>Ca</sub> β subunit function during diabetes, protein expression of the pore forming BK<sub>Ca</sub> α subunit and BK<sub>Ca</sub> β1 subunit were examined using Western blot analysis. Antibodies were validated for specificity using HEK293 cells expressing either BK<sub>Ca</sub> α or BK<sub>Ca</sub> β1 subunits (Fig. 6A and Supplementary Fig. S1). Bands of similar molecular weight for the BK<sub>Ca</sub> α subunit were found in lysates from HEK293 cells stably expressing this subunit and human adipose arteries (Fig. 6A). The molecular weight of the BK<sub>Ca</sub> β1 subunit was slightly higher in lysates from human adipose arteries compared to HEK293 cell transfected with a BK<sub>Ca</sub> β1 construct (Fig. 6A), perhaps reflecting differences in post-translational modifications as recently observed<sup>29</sup>. A non-specific band of ~40 kDa was observed in lysates from HEK cells, but only cells expressing BK<sub>Ca</sub> β1 showed the expected immunoreactive band at 25 kDa (Fig. 6A and Supplementary Figs S1A and S2A). Also note that only one immunoreactive band of expected molecular weight for the BK<sub>Ca</sub> β1 was detected in human adipose arterial lysates (Supplementary Figs S1B and S2A).

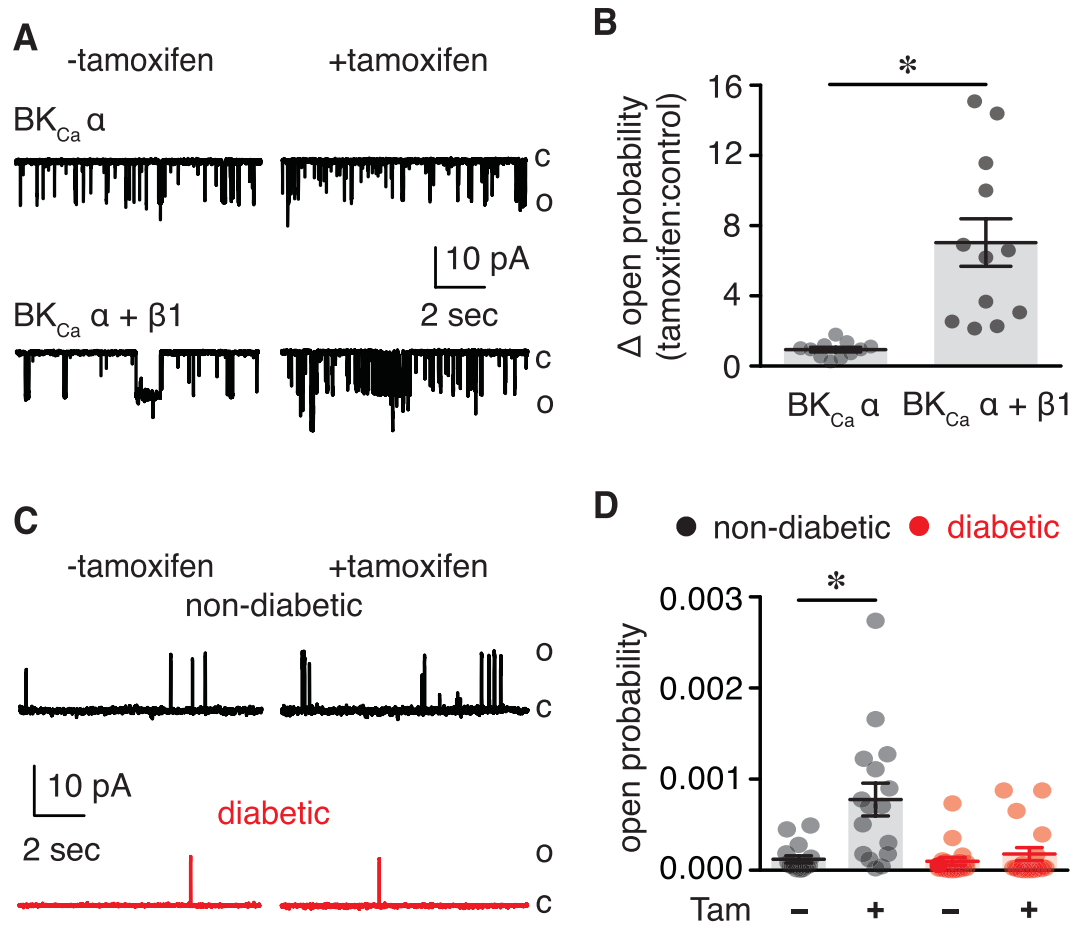


**Figure 5.** Impaired BK<sub>Ca</sub> β1 subunit function in human diabetic vascular smooth muscle. **(A)** Representative single BK<sub>Ca</sub> channel records at +40 mV and 1 μM free Ca<sup>2+</sup> obtained from excised membrane patches of HEK293 cells expressing only BK<sub>Ca</sub> α subunit or coexpressing BK<sub>Ca</sub> α + BK<sub>Ca</sub> β1 subunits in the absence and presence of tamoxifen (1 μM). **(B)** Bar plot summarizing the change in open probability (tamoxifen: control) for HEK293 cells expressing BK<sub>Ca</sub> α (n = 11 cells) or BK<sub>Ca</sub> α + BK<sub>Ca</sub> β1 (n = 12 cells) subunits. \**P* < 0.05, unpaired *t* test. **(C)** Representative single BK<sub>Ca</sub> channel traces recorded from excised membrane patches of vascular smooth muscle from non-diabetic and diabetic patients with 1 μM free Ca<sup>2+</sup> in the bath before (–) and after (+) application of 1 μM tamoxifen. **(D)** Amalgamated data summarizing BK<sub>Ca</sub> open probability in non-diabetic (n = 17 cells, 9 subjects) and diabetic (n = 19 cells, 8 subjects) cells in the presence or absence of tamoxifen. (C: closed; O: open) \**P* < 0.05, Wilcoxon test. Significance for Fig. 5B was compared between cells co-expressing BK<sub>Ca</sub> α + BK<sub>Ca</sub> β1 vs. BK<sub>Ca</sub> α only. Significance for Fig. 5D was compared to corresponding - tamoxifen datasets.

Subsequent examination of total protein abundance for BK<sub>Ca</sub> α and BK<sub>Ca</sub> β1 subunits in human non-diabetic and diabetic arteries revealed no differences between groups (Fig. 6B and C).

To further explore mechanisms that may contribute to compromised BK<sub>Ca</sub> channel activity and BK<sub>Ca</sub> β1 subunit function during diabetes, the coupling between BK<sub>Ca</sub> α and BK<sub>Ca</sub> β1 was examined using Proximity Ligation Assay (PLA)<sup>30</sup> and immunofluorescence analysis. PLA fluorescent puncta are generated when proteins of interest are 40 nm or less apart. PLA signals were negligible when primary antibodies for BK<sub>Ca</sub> α and/or BK<sub>Ca</sub> β1 subunits were omitted from the preparation (Fig. 7A,B,C and H). As a positive control, vascular smooth muscle from non-diabetic and diabetic subjects stained with two different BK<sub>Ca</sub> α subunit antibodies demonstrated robust PLA signals with similar number of PLA puncta (Fig. 7D,E and H). In vascular smooth muscle co-labeled for BK<sub>Ca</sub> α and BK<sub>Ca</sub> β1, data revealed a significant reduction in PLA puncta in diabetic cells compared to non-diabetic cells (Fig. 7F,G and H). Immunofluorescence analysis showed strong BK<sub>Ca</sub> α-associated immunofluorescence of similar intensity (normalized to cytosol) along the plasma membrane of non-diabetic (1.7 ± 0.1) and diabetic (1.6 ± 0.1) vascular smooth muscle (*P* = 0.460; Mann Whitney Test; Supplementary Fig. S3). Conversely, the intensity of the BK<sub>Ca</sub> β1-associated fluorescence along the plasma membrane was markedly reduced in diabetic cells (0.8 ± 0.1) compared to non-diabetic cells (1.5 ± 0.1; *P* < 0.05; Mann Whitney Test; Supplementary Fig. S3). Altogether, these results suggest that BK<sub>Ca</sub> β1-mediated regulation of BK<sub>Ca</sub> channels may be compromised in vascular smooth muscle from adipose arteries of diabetic patients due to suppressed functional coupling between BK<sub>Ca</sub> α and BK<sub>Ca</sub> β1 subunits, rather than a reduction in cellular subunit abundance.



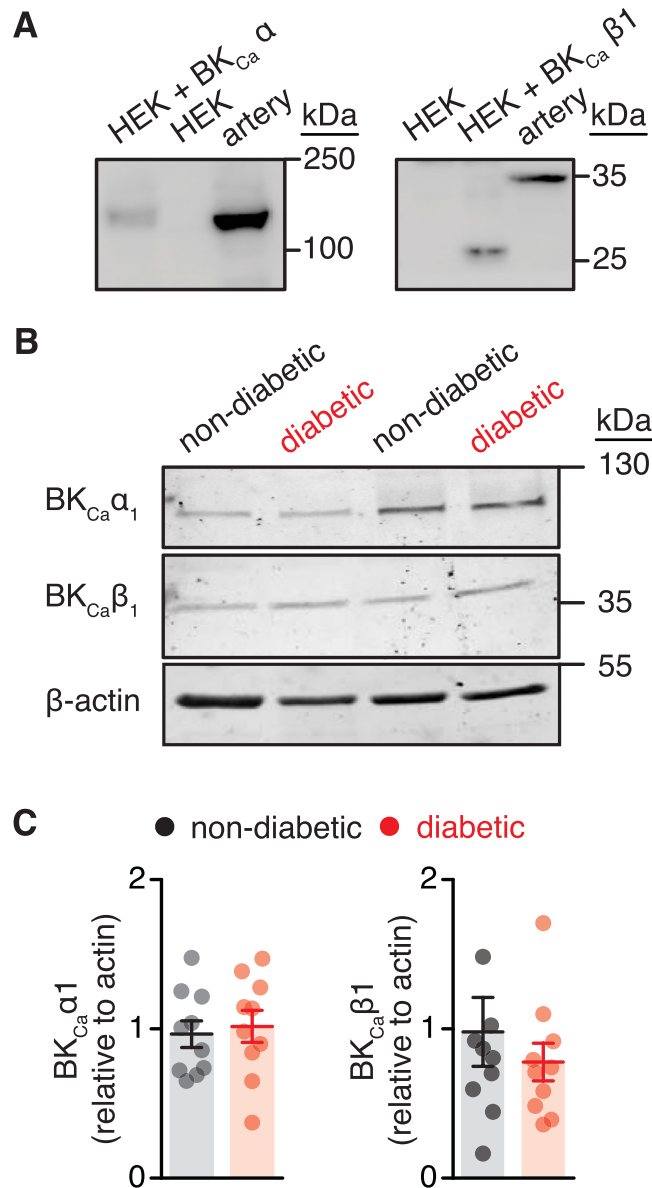


**Figure 6.** No change in BK<sub>Ca</sub> subunit total protein levels in arterial lysates from non-diabetic and diabetic patients. **(A)** Representative immunoreactive bands corresponding to BK<sub>Ca</sub> α<sub>1</sub> and BK<sub>Ca</sub> β<sub>1</sub> subunits in lysates from untransfected HEK293 cells (HEK), HEK293 cells transfected with either BK<sub>Ca</sub> α<sub>1</sub> or BK<sub>Ca</sub> β<sub>1</sub> subunit and human arteries from non-diabetic patients (n = 3 lysates per condition). Full-length blots are shown in Supplementary Fig. S2A. **(B)** Representative immunoreactive bands corresponding to BK<sub>Ca</sub> α<sub>1</sub> and BK<sub>Ca</sub> β<sub>1</sub> subunits, and β-actin as a normalization control. Full-length blots are shown in Supplementary Fig. S2B. **(C)** Corresponding densitometric summary data for each subunit obtained using arterial lysates from non-diabetic (n = 10 lysates) and diabetic (n = 10 lysates) patients. \*P < 0.05, Mann-Whitney test. Significance was compared between non-diabetic and diabetic datasets.

## Discussion

In this study we report three major novel findings related to BK<sub>Ca</sub> channels in native small diameter adipose arteries and vascular smooth muscle cells from non-diabetic and type 2 diabetic patients. First, BK<sub>Ca</sub> channel activity acts to oppose pressure-induced constriction in isolated human resistance adipose arteries, but this is compromised in arteries from diabetic patients. Second, BK<sub>Ca</sub> channel activity is impaired in vascular smooth muscle from diabetic patients, as reflected by reduced apparent Ca<sup>2+</sup> sensitivity, dwell open time and BK<sub>Ca</sub> β subunit function. Third, compromised BK<sub>Ca</sub> β subunit function during diabetes is not associated with changes in total protein abundance of this subunit, but rather seems to be the result of a reduction in the association/coupling between BK<sub>Ca</sub> α and BK<sub>Ca</sub> β<sub>1</sub> subunits. The implications of these changes are significant as they may impact vascular reactivity and/or contribute to vascular complications in humans with type 2 diabetes, independent of changes in endothelial function<sup>6,24,31–33</sup>.



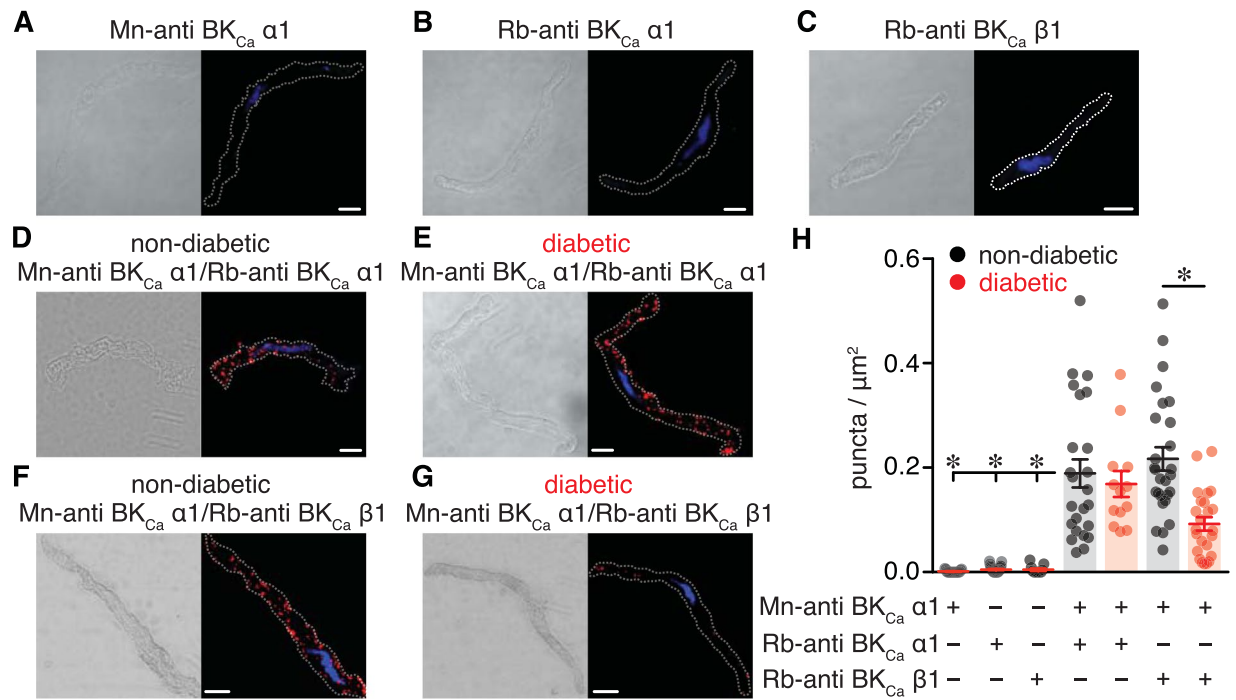


**Figure 7.** Decreased association between BK<sub>Ca</sub> α1 and BK<sub>Ca</sub> β1 subunits in vascular smooth muscle cells from diabetic patients. (A–C) Differential interference contrast (DIC) and confocal fluorescent PLA puncta (red) and DAPI (blue) images of freshly dissociated human vascular smooth muscle cells labeled with mouse-anti BK<sub>Ca</sub> α1 (A), rabbit-anti BK<sub>Ca</sub> α1 (B), and rabbit-anti BK<sub>Ca</sub> β1 (C) antibodies. (D,E) DIC (left) and fluorescence PLA (red)/DAPI (blue) (right) images of dissociated vascular smooth muscle from non-diabetic (D) and diabetic (E) patients co-labeled with two distinct antibodies for the BK<sub>Ca</sub> α1 subunit. (F,G) DIC (left) and fluorescence PLA (red)/DAPI (blue) (right) images of dissociated human vascular smooth muscle from non-diabetic (F) and diabetic (G) patients co-labeled for BK<sub>Ca</sub> α1 and BK<sub>Ca</sub> β1 subunits. Scale bar = 10 μm. (H) Quantification of PLA fluorescent puncta per μm<sup>2</sup> cell area for non-diabetic and diabetic vascular smooth muscle cells labeled for mouse-anti BK<sub>Ca</sub> α1 (n = 19 cells), rabbit-anti BK<sub>Ca</sub> α1 (n = 27 cells), rabbit-anti BK<sub>Ca</sub> β1 (n = 12 cells), mouse-anti BK<sub>Ca</sub> α1 + rabbit-anti BK<sub>Ca</sub> α1 (n = 24 non-diabetic, 14 diabetic cells); mouse-anti BK<sub>Ca</sub> α1 + rabbit-anti BK<sub>Ca</sub> β1 (n = 27 non-diabetic, 24 diabetic cells). \*P < 0.05, Mann-Whitney test. Significance for columns 1, 2, 3 and 5 was compared to column 4, and column 7 was compared to column 6.

Results of experiments examining the effects of IbTx on arterial tone suggest that BK<sub>Ca</sub> channels serve an important physiological role to oppose pressure-induced vasoconstriction in human adipose arteries, but become severely compromised in adipose arteries from diabetic patients (Fig. 1). These results suggest that BK<sub>Ca</sub> channel function is compromised in adipose arteries from humans with diabetes. Consistent with this, BK<sub>Ca</sub>-mediated STOCs amplitude and frequency as well as single BK<sub>Ca</sub> channel function were significantly reduced in dissociated vascular smooth muscle from adipose arteries from diabetic subjects (Figs 2 and 4). Similar results were observed in a number of studies using vascular smooth muscle from several vascular beds and different animal models of diabetes<sup>9,21–23,25,34</sup>. A reduction in BK<sub>Ca</sub> channel activity and BK<sub>Ca</sub> β1 function may also contribute to vascular complications by aggravating vessel wall remodeling and fibrosis during diabetes<sup>35</sup>. Thus, a potential common BK<sub>Ca</sub>-mediated mechanism contributing to vascular complications during diabetes may be engaged in a variety of species. In animal models of diabetes, alterations in BK<sub>Ca</sub> channel function have been associated, in part, to changes in the activity of Ca<sup>2+</sup> sparks<sup>21,22,25</sup>. Here, no changes in Ca<sup>2+</sup> sparks properties were detected between dissociated vascular smooth muscle from adipose arteries from non-diabetic and diabetic patients (Fig. 3). These results are similar to those found in vascular smooth muscle from high fat diet mice in which Ca<sup>2+</sup> spark activity was unaffected compared to cells from low fat fed mice<sup>9</sup>. Discrepancies with other studies could arise from experimental conditions, use of smooth muscle from different vascular beds, or intrinsic differences between murine and human cells/tissue<sup>31,36</sup>. Regardless, our results implicate other mechanisms as culprit for compromised BK<sub>Ca</sub> channel activity in human vascular smooth muscle during diabetes.

The accessory BK<sub>Ca</sub> β1 subunit finely tunes the activity of BK<sub>Ca</sub> channels in vascular smooth muscle by increasing their voltage- and calcium-sensitivity<sup>27</sup>. Impaired BK<sub>Ca</sub> channel function has been associated with suppression of BK<sub>Ca</sub> β1 subunit function in several studies with animal models of diabetes<sup>9,21–23,25</sup>. Moreover, compromised BK<sub>Ca</sub> channel activity was linked with suppression of BK<sub>Ca</sub> β1 subunit function in human vascular smooth muscle from Han Chinese patients with hypertension<sup>24</sup>. We found that BK<sub>Ca</sub> β1 subunit function was significantly suppressed in diabetic vascular smooth muscle from adipose tissue as assessed by tamoxifen sensitivity (Figs 4 and 5). Note that consistent with experiments here (Fig. 5), several groups including ours have validated and confirmed that the effects of tamoxifen on BK<sub>Ca</sub> channels require the presence of the BK<sub>Ca</sub> β1 subunit<sup>9,19,28</sup>. The impairment in BK<sub>Ca</sub> β1 subunit function helps explain the reduced apparent Ca<sup>2+</sup> sensitivity and dwell open time of BK<sub>Ca</sub>

channels as well as the blunted IBTx-induced constriction in diabetic compared to non-diabetic vascular smooth muscle cells/adipose arteries. The loss of BK<sub>Ca</sub>  $\beta$ 1 subunit function in animal models of diabetes<sup>9,21–23,25</sup> and in humans with hypertension<sup>24</sup> has been mainly attributed to transcriptional and/or post-translational changes in BK<sub>Ca</sub>  $\beta$ 1 subunit expression. In contrast with these seemingly consistent molecular mechanisms, no changes in total BK<sub>Ca</sub>  $\alpha$  and BK<sub>Ca</sub>  $\beta$ 1 protein levels were detected between non-diabetic and diabetic arterial lysates (Fig. 6). Rather, PLA data revealed a reduced association between BK<sub>Ca</sub>  $\alpha$  and BK<sub>Ca</sub>  $\beta$ 1 subunits in diabetic cells compared to non-diabetic cells (Fig. 7). Furthermore, immunofluorescence imaging provided evidence of a decreased surface expression of BK<sub>Ca</sub>  $\beta$ 1, but not BK<sub>Ca</sub>  $\alpha$ , in diabetic cells compared to non-diabetic cells (Supplementary Fig. S2). This is important as recent studies have suggested that dynamic trafficking of the BK<sub>Ca</sub>  $\beta$ 1 subunit to the plasma membrane is essential for coupling with the mostly membrane bound, pore forming BK<sub>Ca</sub>  $\alpha$  subunit in vascular smooth muscle<sup>37,38</sup>. This dynamic interaction between BK<sub>Ca</sub> subunits contributes to vascular reactivity under basal conditions<sup>37</sup> and in response to chronic angiotensin II signaling<sup>38</sup>. Also note that a recent study using human vascular smooth muscle has shown that changes in K<sub>V</sub>1.5 surface expression (perhaps due to altered trafficking of the subunit) rather than differences in total protein levels has been associated with impaired K<sub>V</sub>1.5 channel and vascular reactivity in humans with coronary artery disease<sup>39</sup>. Thus, it is tempting to speculate, for future studies, that a change in BK<sub>Ca</sub>  $\beta$ 1 subunit trafficking may contribute to compromised BK<sub>Ca</sub> channel activity and vascular reactivity in humans with diabetes.

Vascular complications during diabetes may also be associated with impairment in the function of other ion channels in vascular smooth muscle. For example, it was recently reported that L-type Ca<sup>2+</sup> channel (LTCC) activity was significantly augmented in vascular smooth muscle from humans with diabetes<sup>40</sup>. This can stimulate Ca<sup>2+</sup> influx to increase global intracellular Ca<sup>2+</sup> in vascular smooth muscle. Interestingly, use of a mathematical model of rodent vascular smooth muscle electrophysiology and Ca<sup>2+</sup> dynamics showed that increased LTCC activity predominantly contributes to impaired intracellular Ca<sup>2+</sup> during diabetic hyperglycemia<sup>41</sup>. Yet, the model also revealed that this effect on global intracellular Ca<sup>2+</sup> is substantially amplified when an increase in LTCC activity is accompanied by a decrease in the activity of potassium (K<sup>+</sup>) channels<sup>41</sup>. Indeed, previous studies have shown a selective suppression in voltage-gated K<sup>+</sup> (K<sub>V</sub>) and BK<sub>Ca</sub> channel activity that is associated with downregulation of K<sub>V</sub>2.1 and BK<sub>Ca</sub>  $\beta$ 1 subunit, respectively, in vascular smooth muscle from diabetic mice on a high fat diet<sup>9,10</sup>. Thus, potentiation of LTCC activation and suppression of K<sup>+</sup> channel activity, including that of BK<sub>Ca</sub> channels as in this study, may synergize to impact vascular reactivity and/or contribute to vascular complications in humans with diabetes. Given the role of K<sub>V</sub> channels in vascular smooth muscle excitability due to their influence on membrane potential, it will be important to examine the function of these channels as well as the individual contributions of different K<sub>V</sub> subunits in human cells during control conditions and in diabetes. Collectively, these data will critically inform the development of novel computational models specific to human vascular smooth muscle. This computational approach may help identify and predict the relative contribution of many elements (i.e. LTCC, K<sub>V</sub> channels, BK<sub>Ca</sub> channels, etc.) that interact non-linearly to control vascular smooth muscle excitability in humans during physiological and pathological conditions.

The use of human tissue from obese non-diabetic and clinically diagnosed type 2 diabetic patients provides unparalleled translational significance. Yet, factors such as underlying environmental factors, biological variables such as sex and age, genetic background, disease progression, prescription history, personal habits (e.g. smoking) and comorbidities may confound results. Despite these limitations, data in this study are internally consistent and reproducible across different experimental approaches. Indeed, we also recently demonstrated high reproducibility in biochemical and electrophysiological outcomes using similar tissue samples<sup>40</sup>. Furthermore, whereas the use of tissue from obese non-diabetic patients is less than ideal as a true “control”, it does highlight the added stress imposed by diabetes in mediating alterations in BK<sub>Ca</sub> channel activity. To conclude, and to the best of our knowledge, this study provides the first direct evidence that compromised BK<sub>Ca</sub> channel activity in native, freshly dissociated vascular smooth muscle may contribute to vascular complications in type 2 diabetic patients. Interestingly, the mechanisms underlying aberrant vascular BK<sub>Ca</sub> channel activity in humans with diabetes follow some, but not all, the molecular features observed in animal models of diabetes. Gathering information from native human cells may be necessary for development of rational strategies to treat vascular complications in humans with type 2 diabetes.

## Methods

**Human Tissue (Study Approval).** Excised adipose arteries from obese patients undergoing surgical sleeve gastrectomy and that were either non-diabetic or clinically diagnosed with type 2 diabetes were used. Samples were obtained after Institutional Review Board (IRB) approval from the University of Nevada Reno School of Medicine (IRB ID: 2013-019) and in accordance with the guidelines of the *Declaration of Helsinki*. The need for informed consent was waived by IRBs at the University of Nevada Reno School of Medicine (IRB ID: 2013-019) and the University of California Davis School of Medicine (IRB ID: 597267-1) because the tissue is considered “waste”, has no codification that could be used to identify patients and was determined not to be human subject research in accordance with United States of America federal regulations, as defined by 45 CFR 46.102(f). This precludes the acquisition of detailed clinical profiles other than sex, age and whether the patient was diabetic or not (see Table S1). Therefore, no exclusions were made due to medication history or presence of comorbidities. Patients were considered diabetic if they had a hemoglobin A-1c level equal to or greater than 6.5% on pre-surgical testing, or if they were on medication for diabetes treatment<sup>42</sup>. Collected tissue was placed in cold phosphate-buffered saline (PBS) solution containing (in mM): 138 NaCl, 3 KCl, 10 Na<sub>2</sub>HPO<sub>4</sub>, 2 NaH<sub>2</sub>PO<sub>4</sub>, 5 D-glucose, 0.1 CaCl<sub>2</sub>, and 0.1 MgSO<sub>4</sub>, pH 7.4 with NaOH until used.

**Vascular Smooth Muscle Cell Isolation.** Single vascular smooth muscle cells were dissociated from small diameter adipose arteries from non-diabetic and type 2 diabetic patients using enzymatic digestion as previously

described<sup>40</sup>. Adipose arteries were dissected in ice-cold dissection buffer composed of (in mM): 140 NaCl, 5 KCl, 2 MgCl<sub>2</sub>, 10 D-glucose, and 10 HEPES, pH 7.4 with NaOH. Following dissection, arteries were cut in small pieces and digested in dissection buffer supplemented with papain (26 U/ml) and dithiothreitol (1 mg/ml) at 37 °C for 15 minutes. After this first incubation period, the solution was exchanged with dissection buffer supplemented with collagenase type H (1.95 U/ml), elastase (0.5 mg/ml) and soybean trypsin Inhibitor (1 mg/ml) at 37 °C for 15 minutes. Cells were then washed in ice-cold dissection buffer three times. Glass pipettes of decreasing diameters were then used to gently triturate arteries and obtain single vascular smooth muscle cells. Isolated cells were maintained in ice-cold dissection buffer until use.

**Arterial Diameter Measurements.** Freshly dissected small diameter adipose arteries were cannulated on glass micropipettes and mounted in a 5 mL myograph chamber (Living Systems Instrumentation, St. Albans, VT) as described previously<sup>9,43,44</sup>. The vessels were pressurized to 20 mmHg and allowed to equilibrate while continuously perfused (37 °C, 30 min, 3–5 mL/min) with physiological saline solution (PSS) consisting of (in mM): 119 NaCl, 4.7 KCl, 2 CaCl<sub>2</sub>, 24 NaHCO<sub>3</sub>, 1.2 KH<sub>2</sub>PO<sub>4</sub>, 1.2 MgSO<sub>4</sub>, 0.023 ethylenediaminetetraacetic acid (EDTA) and 10 D-glucose aerated with 5% CO<sub>2</sub>/95% O<sub>2</sub>, pH 7.35–7.40. Following an equilibration period, arteries were treated with 60 mM KCl (<5 min; isosmotic replacement of NaCl with KCl) to test their viability. Only arteries with ≥50% constriction in response to 60 mM KCl were used for subsequent experiments. Intravascular pressure was increased to 80 mmHg and arteries were allowed to develop myogenic tone. Lumen diameters of the adipose arteries were recorded using IonOptix software (IonOptix LLC, Westwood-MA). To evaluate the impact of BK<sub>Ca</sub> channels on myogenic tone, arteries were treated with 100 nM Iberiotoxin (IBTx) (BK<sub>Ca</sub> channel inhibitor). Percent change in diameter was calculated using the following equation: % myogenic tone = [(DP – DA)/DP] × 100, where DP = passive diameter of the artery in Ca<sup>2+</sup>-free PSS containing the L-type Ca<sup>2+</sup> channel (LTCC) inhibitor nifedipine (10 μM) and DA = active diameter of the artery in Ca<sup>2+</sup>-containing PSS. Percent constriction in the presence of IBrTx or 60 mM K<sup>+</sup> was calculated using the following equation: % constriction = [(DP – DT)/DP] × 100, where DT = diameter of the artery in Ca<sup>2+</sup>-containing PSS with 100 nM IBrTx or 60 mM K<sup>+</sup> and DP = passive diameter of the artery in Ca<sup>2+</sup>-free PSS containing 10 μM of the LTCC inhibitor nifedipine.

**Electrophysiology.** STOCs resulting from the concerted opening of multiple BK<sub>Ca</sub> channels were recorded at different membrane potentials from freshly dissociated vascular smooth muscle from small diameter adipose arteries using the perforated whole-cell configuration of the patch-clamp technique with an Axopatch 200B amplifier (Molecular Devices, Sunnyvale, CA). Currents were sampled at 10 kHz and low-pass filtered at 2 kHz. The pipette solution consisted of (in mM): 110 K-aspartate, 30 KCl, 10 NaCl, 1 MgCl<sub>2</sub>, 0.5 EGTA, and 10 HEPES, pH adjusted to 7.3 with KOH. The pipette solution was supplemented with 250 μg/ml of amphotericin B (Sigma, St. Louis, MO). Bath solution consisted of (in mM): 130 NaCl, 5 KCl, 2 CaCl<sub>2</sub>, 1 MgCl<sub>2</sub>, 10 glucose and 10 HEPES, pH adjusted to 7.4 with NaOH. STOCs were analyzed using the threshold detection algorithm in Clampfit 10 (Axon Instruments, Inc).

Single BK<sub>Ca</sub> channel currents were recorded from inside-out membrane patches obtained from freshly dissociated vascular smooth muscle cells from adipose arteries. In some experiments, HEK293 cells expressing either the BK<sub>Ca</sub> α subunit and EGFP or co-transfected with BK<sub>Ca</sub> α + β1 subunit in a 1:1 mix and EGFP using PolyPlus jetPRIME were used as previously described<sup>9</sup>. Bath and pipette solutions consisted of (in mM) 140 KCl, 1 HEDTA, 10 HEPES, pH adjusted to 7.3 with Tris. Bath solution was supplemented with CaCl<sub>2</sub> to achieve the desired free Ca<sup>2+</sup> concentration, as determined with the MaxChelator software. Single-channel currents were amplified, low-pass filtered at 1 kHz, and sampled at 20 kHz with the Axopatch 200B amplifier using a DigiData 1440 A acquisition board and pClamp 10 software (Axon Instruments, Inc). Currents were elicited by holding the inside-out patch at the specified voltage. Data were directly stored in a PC hard drive. The half-amplitude algorithm of Clampfit 10 was used to detect single-channel openings and to analyze data of channel activity (e.g. open probability; P<sub>o</sub>). The number of BK<sub>Ca</sub> channels per patch was estimated by holding the patch at +80 mV in the presence of 10 μM free Ca<sup>2+</sup>, which maximizes the P<sub>o</sub> of these channels<sup>45</sup>. Open time histograms were fit using a log-normal function:

$$y = A \cdot e^{\frac{-\{[\ln(x) - \ln(\tau)]^2\}}{2\sigma^2}}$$

where A is a constant, τ is the time constant, and σ is the standard deviations of τ. This analysis was validated by using an Akaike's Information Criterion, which determines the probability that a data set could be described by a particular set of competing models<sup>46</sup>.

**Ca<sup>2+</sup> Imaging and Analysis.** Freshly dissociated vascular smooth muscle cells from small diameter adipose arteries were loaded with the fluorescent Ca<sup>2+</sup> indicator fluo-4 AM (5 μM) and imaged using an Andor spinning disk confocal microscope system coupled to an Olympus iX81 inverted microscope equipped with a 60x oil immersion lens (numerical aperture 1.49). Andor IQ software was used for acquisition. Images were acquired at 100–120 Hz. Analysis was performed using custom software (SparkLab) written in LabVIEW that employs a computer algorithm as previously described<sup>9,47</sup>.

**Proximity Ligation Assay (PLA).** The Duolink *in situ* PLA detection kit was used to determine colocalization between BK<sub>Ca</sub> α and BK<sub>Ca</sub> β1 subunits as previously described<sup>40</sup>. Freshly dissociated myocytes were plated on glass coverslips and allowed to sit for 30 minutes at room temperature. Cells were then fixed in 4% paraformaldehyde (20 min) and quenched in 100 mM glycine (15 min), followed by 3 min washes (2x) in a phosphate-buffered saline (PBS) solution containing (in mM) 138 NaCl, 3 KCl, 10 Na<sub>2</sub>HPO<sub>4</sub>, 2 NaH<sub>2</sub>PO<sub>4</sub>, 5 D-glucose, 0.1 CaCl<sub>2</sub> and 0.1 MgSO<sub>4</sub>, pH adjusted to 7.4 with NaOH. Cells were then permeabilized for 20 minutes in 0.1% Triton-100

solution in PBS and blocked in Duolink Blocking Solution for 1 hour at 37 °C in a humidity chamber. Cells were incubated overnight with a specific combination of primary antibodies. Mouse anti-BK<sub>Ca</sub> α (Antibodies Inc; 75–022 1:200) was combined with rabbit anti-BK<sub>Ca</sub> β1 (Abcam; ab3587; 1:200) antibody. As a positive control, cells were stained with mouse anti-BK<sub>Ca</sub> α (Antibodies Inc; 75–022 1:200) and rabbit anti-BK<sub>Ca</sub> α (Alomone; APC-021; 1:200). For negative controls, cells were incubated with only one primary antibody. Antibodies were diluted in Duolink Antibody Diluent Solution per manufacturer instructions. Secondary antibodies containing PLA probes (anti-mouse minus and anti-rabbit plus) were added to the preparation and allowed to incubate for 1 h at 37 °C. A ligation solution consisting of ligase and two distinct oligonucleotides was then added and incubated for 30 minutes at 37 °C. This step was followed by an amplification reaction (100 min, 37 °C), and subsequent washes (2x) for 10 minutes in Duolink Buffer B and 1 × 1 minute in 1% Buffer B per manufacturer's specifications. Coverslips were mounted on a microscope slide with Duolink mounting media. The fluorescence signal was visualized using an Olympus FV1000 confocal system on an Olympus iX81 microscope with a 60X water immersion lens (numerical aperture = 1.4). Images were acquired at different optical planes (z-axis step size = 0.5 μm).

**Immunofluorescence.** Immunofluorescence labeling of freshly dissociated vascular smooth muscle from small diameter adipose arteries from non-diabetic and diabetic patients was performed as described previously<sup>10,48</sup> using a rabbit anti-BK<sub>Ca</sub> α (Alomone; APC-021; 1:200) and a rabbit anti-BK<sub>Ca</sub> β1 (Abcam; ab3587; 1:200). The secondary antibody was an Alexa Fluor 568-conjugated donkey anti-rabbit (5 mg/mL) from Molecular Probes. Cells were visualized (512 × 512 pixel images) using an Olympus FV1000 confocal microscope coupled with an Olympus X60 water immersion lens (NA = 1.4) and a zoom of 3.5 (pixel size = 0.1 μm). Images were collected at multiple optical planes (z axis step size = 0.25 μm). The specificity of the primary antibody was tested in negative control experiments in which the primary antibody was substituted with PBS. Cells for each group were imaged using the same laser power, gain settings and pinhole for all treatments.

**Western Blot Analysis.** Whole tissue homogenates were prepared from dissected adipose arteries. In some experiments, protein lysates were obtained from HEK293 cells expressing either the BK<sub>Ca</sub> α or BK<sub>Ca</sub> β1 subunit or cells that have not been transfected. Samples were flash frozen in liquid nitrogen and homogenized on ice with lysis buffer containing (in mM) 150 NaCl, 10 Na<sub>2</sub>HPO<sub>4</sub>, 1 EDTA with 1% deoxycholic acid, 0.1% sodium dodecyl sulfate, 40 β-glycerophosphate, 20 Na pyrophosphate, 30 NaF, 1 dithiothreitol and protease inhibitors (Complete Mini protease inhibitor cocktail, Roche, San Francisco, CA) in a glass dounce homogenizer. Whole lysates were sonicated for 1 min, rested on ice for 20 min, and centrifuged (5000 rpm, 4 °C) to yield clarified supernatant. Equal amounts of protein (approximately 10 μg) were separated under reducing conditions on a 4–20% gradient polyacrylamide gel according to the manufacturer's specifications (Bio-Rad, Hercules, CA). Proteins were transferred to polyvinylidene difluoride (PVDF) or nitrocellulose membranes for Western immunoblotting using enhanced chemiluminescence (ECL) and X-ray film or using an Odyssey scanner (LI-COR; Lincoln, NE, USA) with far red or near-infrared (NIR) labeled secondary antibodies. For the Odyssey scanner, nitrocellulose membranes were blocked with 50% Odyssey blocking buffer (LI-COR; Lincoln, NE, USA) (40 min) in Tris-buffered saline (TBS), then incubated with BK<sub>Ca</sub> subunit specific primary antibodies on a rotating platform for 18–24 h (4 °C). Primary antibodies were rabbit anti-BK<sub>Ca</sub> α (Alomone; APC-021; 1:500), rabbit anti-BK<sub>Ca</sub> β1 (Genetex; GTX105666; 1:5000; or Abcam; ab3587; 1:500), anti-BK<sub>Ca</sub> γ (Alomone; APC-021; 1:500), and mouse anti-β actin (Sigma; AC-40; 1:4000; as a loading control). These antibodies were diluted in TBS with 0.05% tween-20 (t) and 5% Odyssey blocking solution. Membranes were washed 3 times in TBS-t, then incubated (2 h, room temperature) with appropriate secondary antibodies: goat anti-rabbit 680LT (LI-COR; 925-68021; 1:15,000; with 0.1% SDS), 800CW (LI-COR; 925-32211; 1:15,000; for dual staining) or goat anti-mouse 680LT (LI-COR; 925-68020 1:10,000) in TBS-t. For the far red or NIR dyes, band images were acquired using an Odyssey scanner. In some experiments, detection of BK<sub>Ca</sub> α was acquired by X-ray film. PVDF membranes were blocked with 10% nonfat milk for 1 hour, incubated in rabbit anti-BK<sub>Ca</sub> α (Alomone; 1:500) for 2 hours, washed 3 times in TBS-t, incubated in HRP labeled goat anti-mouse (sc-2005; 1:5000; Santa Cruz), then washed 3 times in TBS-t. Bands were identified by ECL and exposure to X-ray film, followed by conventional scanning. Densitometry for immunoreactive bands was performed with ImageJ software (National Institutes of Health). Band quantification was normalized to β actin, and expressed as a percentage of control.

**Chemicals and Statistics.** All chemical reagents were from Sigma-Aldrich (St. Louis, MO) unless otherwise stated. Iberiotoxin was from Peptides International (Louisville, KY). Data were analyzed using GraphPad Prism software and expressed as mean ± SEM. Data were assessed for potential outliers using the GraphPad Prism Outlier Test and for normality of distribution using the Shapiro-Wilk or KS normality tests. Statistical significance was then determined using appropriate paired or unpaired Student's *t*-test, nonparametric tests or One-way analysis of variance (ANOVA) for multiple comparisons with appropriate post hoc test. *P* < 0.05 was considered statistically significant (denoted by \* in figures).

**Data Availability.** The datasets generated during and/or analyzed during the current study are available from the corresponding author in a reasonable request.

## References

1. WHO. <http://www.who.int/mediacentre/factsheets/fs312/en/index.html> (2011).
2. Cooper, M. E., Bonnet, F., Oldfield, M. & Jandeleit-Dahm, K. Mechanisms of diabetic vasculopathy: an overview. *Am J Hypertens* **14**, 475–486 (2001).
3. Sonoyama, K., Greenstein, A., Price, A., Khavandi, K. & Heagerty, T. Vascular remodeling: implications for small artery function and target organ damage. *Therapeutic advances in cardiovascular disease* **1**, 129–137 (2007).
4. Aronson, D. Hyperglycemia and the pathobiology of diabetic complications. *Adv Cardiol* **45**, 1–16 (2008).



5. Brown, A., Reynolds, L. R. & Bruemmer, D. Intensive glycemic control and cardiovascular disease: an update. *Nature reviews. Cardiology* **7**, 369–375 (2010).
6. Schofield, I., Malik, R., Izzard, A., Austin, C. & Heagerty, A. Vascular structural and functional changes in type 2 diabetes mellitus: evidence for the roles of abnormal myogenic responsiveness and dyslipidemia. *Circulation* **106**, 3037–3043 (2002).
7. Williams, S. B., Cusco, J. A., Roddy, M. A., Johnstone, M. T. & Creager, M. A. Impaired nitric oxide-mediated vasodilation in patients with non-insulin-dependent diabetes mellitus. *Journal of the American College of Cardiology* **27**, 567–574 (1996).
8. Montero, D. *et al.* Vascular smooth muscle function in type 2 diabetes mellitus: a systematic review and meta-analysis. *Diabetologia* **56**, 2122–2133 (2013).
9. Nystoriak, M. A. *et al.* AKAP150 Contributes to Enhanced Vascular Tone by Facilitating Large-Conductance  $\text{Ca}^{2+}$ -Activated  $\text{K}^{+}$  Channel Remodeling in Hyperglycemia and Diabetes Mellitus. *Circ Res* **114**, 607–615 (2014).
10. Nieves-Cintrón, M. *et al.* Selective downregulation of  $\text{Kv}2.1$  function contributes to enhanced arterial tone during diabetes. *Journal of Biological Chemistry* **290**, 7918–7929 (2015).
11. Navedo, M. F., Takeda, Y., Nieves-Cintrón, M., Molkentin, J. D. & Santana, L. F. Elevated  $\text{Ca}^{2+}$  sparklet activity during acute hyperglycemia and diabetes in cerebral arterial smooth muscle cells. *American journal of physiology. Cell physiology* **298**, C211–220 (2010).
12. Jackson, W. F. Ion channels and vascular tone. *Hypertension* **35**, 173–178 (2000).
13. Jaggar, J. H. *et al.*  $\text{Ca}^{2+}$  channels, ryanodine receptors and  $\text{Ca}^{2+}$ -activated  $\text{K}^{+}$  channels: a functional unit for regulating arterial tone. *Acta Physiol Scand* **164**, 577–587 (1998).
14. Amberg, G. C. & Navedo, M. F. Calcium dynamics in vascular smooth muscle. *Microcirculation* **20**, 281–289 (2013).
15. Nelson, M. T. *et al.* Relaxation of arterial smooth muscle by calcium sparks. *Science* **270**, 633–637 (1995).
16. Patterson, A. J., Henrie-Olson, J. & Brenner, R. Vasoregulation at the molecular level: a role for the  $\beta 1$  subunit of the calcium-activated potassium (BK) channel. *Trends Cardiovasc Med* **12**, 78–82 (2002).
17. Brenner, R. *et al.* Vasoregulation by the  $\beta 1$  subunit of the calcium-activated potassium channel. *Nature* **407**, 870–876 (2000).
18. Nieves-Cintrón, M., Amberg, G. C., Nichols, C. B., Molkentin, J. D. & Santana, L. F. Activation of NFATc3 Down-regulates the  $\beta 1$  Subunit of Large Conductance, Calcium-activated  $\text{K}^{+}$  Channels in Arterial Smooth Muscle and Contributes to Hypertension. *J Biol Chem* **282**, 3231–3240 (2007).
19. Amberg, G. C. & Santana, L. F. Downregulation of the BK channel  $\beta 1$  subunit in genetic hypertension. *Circ Res* **93**, 965–971 (2003).
20. Amberg, G. C., Bonev, A. D., Rossow, C. F., Nelson, M. T. & Santana, L. F. Modulation of the molecular composition of large conductance,  $\text{Ca}^{2+}$  activated  $\text{K}^{+}$  channels in vascular smooth muscle during hypertension. *J Clin Invest* **112**, 717–724 (2003).
21. Dong, L. *et al.* Functional and molecular evidence for impairment of calcium-activated potassium channels in type-1 diabetic cerebral artery smooth muscle cells. *Journal of cerebral blood flow and metabolism: official journal of the International Society of Cerebral Blood Flow and Metabolism* **28**, 377–386 (2008).
22. Rueda, A., Fernandez-Velasco, M., Benitah, J. P. & Gomez, A. M. Abnormal  $\text{Ca}^{2+}$  spark/STOC coupling in cerebral artery smooth muscle cells of obese type 2 diabetic mice. *PLoS One* **8**, e53321 (2013).
23. Lu, T. *et al.* Impaired  $\text{Ca}^{2+}$ -dependent activation of large-conductance  $\text{Ca}^{2+}$ -activated  $\text{K}^{+}$  channels in the coronary artery smooth muscle cells of Zucker Diabetic Fatty rats. *Biophys J* **95**, 5165–5177 (2008).
24. Yang, Y. *et al.* Function of BKCa channels is reduced in human vascular smooth muscle cells from Han Chinese patients with hypertension. *Hypertension* **61**, 519–525 (2013).
25. McGahon, M. K. *et al.* Diabetes downregulates large-conductance  $\text{Ca}^{2+}$ -activated potassium  $\beta 1$  channel subunit in retinal arteriolar smooth muscle. *Circ Res* **100**, 703–711 (2007).
26. Bolton, T. B. & Imaizumi, Y. Spontaneous transient outward currents in smooth muscle cells. *Cell Calcium* **20**, 141–152 (1996).
27. Tanaka, Y., Meera, P., Song, M., Knaus, H. G. & Toro, L. Molecular constituents of maxi  $\text{K}_{\text{Ca}}$  channels in human coronary smooth muscle: predominant  $\alpha + \beta$  subunit complexes. *J Physiol* **502**(Pt 3), 545–557 (1997).
28. Dick, G. M. & Sanders, K. M. (Xeno)estrogen sensitivity of smooth muscle BK channels conferred by the regulatory  $\beta 1$  subunit: a study of  $\beta 1$  knockout mice. *J Biol Chem* **276**, 44835–44840 (2001).
29. Detweiler, N. D. *et al.* BK channels in rat and human pulmonary smooth muscle cells are BK $\alpha$ - $\beta 1$  functional complexes lacking the oxygen-sensitive stress axis regulated exon insert. *Pulmonary circulation* **6**, 563–575 (2016).
30. Fredriksson, S. *et al.* Protein detection using proximity-dependent DNA ligation assays. *Nature biotechnology* **20**, 473–477 (2002).
31. Wellman, G. C. *et al.*  $\text{Ca}^{2+}$  sparks and their function in human cerebral arteries. *Stroke* **33**, 802–808 (2002).
32. Hempelmann, R. G., Seebeck, J., Ziegler, A. & Mehdorn, H. M. Effects of potassium channel inhibitors on the relaxation induced by the nitric oxide donor diethylamine nitric oxide in isolated human cerebral arteries. *Journal of neurosurgery* **93**, 1048–1054 (2000).
33. Gokina, N. I. *et al.* Role of  $\text{Ca}^{2+}$ -activated  $\text{K}^{+}$  channels in the regulation of membrane potential and tone of smooth muscle in human pial arteries. *Circ Res* **79**, 881–886 (1996).
34. Howitt, L. *et al.* Differential effects of diet-induced obesity on BKCa  $\{\beta 1\}$ -subunit expression and function in rat skeletal muscle arterioles and small cerebral arteries. *Am J Physiol Heart Circ Physiol* **301**, H29–40 (2011).
35. Xu, H. *et al.* BK channel  $\beta 1$ -subunit deficiency exacerbates vascular fibrosis and remodelling but does not promote hypertension in high-fat fed obesity in mice. *Journal of hypertension* **33**, 1611–1623 (2015).
36. ZhuGe, R. *et al.* Dynamics of signaling between  $\text{Ca}^{2+}$  sparks and  $\text{Ca}^{2+}$ -activated  $\text{K}^{+}$  channels studied with a novel image-based method for direct intracellular measurement of ryanodine receptor  $\text{Ca}^{2+}$  current. *J Gen Physiol* **116**, 845–864 (2000).
37. Leo, M. D. *et al.* Dynamic regulation of  $\beta 1$  subunit trafficking controls vascular contractility. *Proc Natl Acad Sci USA* **111**, 2361–2366 (2014).
38. Leo, M. D. *et al.* Angiotensin II stimulates internalization and degradation of arterial myocyte plasma membrane BK channels to induce vasoconstriction. *Am J Physiol Cell Physiol* **309**, C392–402 (2015).
39. Nishijima, Y. *et al.* Contribution of  $\text{KV}1.5$  Channel to Hydrogen Peroxide-Induced Human Arteriolar Dilation and Its Modulation by Coronary Artery Disease. *Circ Res* **120**, 658–669 (2017).
40. Nystoriak, M. A. *et al.* Ser1928 phosphorylation by PKA stimulates L-type  $\text{Ca}^{2+}$  channel  $\text{Cav}1.2$  and vasoconstriction during acute hyperglycemia and diabetes. *Science signaling* **10** (2017).
41. Morotti, S., Nieves-Cintrón, M., Nystoriak, M. A., Navedo, M. F. & Grandi, E. Predominant contribution of L-type  $\text{Cav}1.2$  channel stimulation to impaired intracellular calcium and cerebral artery vasoconstriction in diabetic hyperglycemia. *Channels*, 1–7 (2017).
42. Association, A. D. Standards of Medical Care in Diabetes - 2017. *Diabetes Care* **40**, S1–S135 (2017).
43. Amberg, G. C., Navedo, M. F., Nieves-Cintrón, M., Molkentin, J. D. & Santana, L. F. Calcium Sparklets Regulate Local and Global Calcium in Murine Arterial Smooth Muscle. *J Physiol* **579**, 187–201 (2007).
44. Nieves-Cintrón, M., Amberg, G. C., Navedo, M. F., Molkentin, J. D. & Santana, L. F. The control of  $\text{Ca}^{2+}$  influx and NFATc3 signaling in arterial smooth muscle during hypertension. *Proc Natl Acad Sci USA* **105**, 15623–15628 (2008).
45. Meera, P., Wallner, M., Jiang, Z. & Toro, L. A calcium switch for the functional coupling between  $\alpha$  (hsl $\alpha$ ) and  $\beta$  subunits ( $\text{K}_{\text{vCa}}$ ) of maxi K channels. *FEBS Lett* **385**, 127–128 (1996).
46. Akaike, H. A new look at the statistical model identification. *IEEE Trans. Autom. Control* **AC19**, 716–723 (1974).
47. Banyasz, T., Chen-Izu, Y., Balke, C. W. & Izu, L. T. A new approach to the detection and statistical classification of  $\text{Ca}^{2+}$  sparks. *Biophys J* **92**, 4458–4465 (2007).
48. Navedo, M. F. *et al.*  $\text{Cav}1.3$  channels produce persistent calcium sparklets, but  $\text{Cav}1.2$  channels are responsible for sparklets in mouse arterial smooth muscle. *Am J Physiol Heart Circ Physiol* **293**, H1359–1370 (2007).

## Acknowledgements

This work was supported by NIH grants R01HL098200 and R01HL121059 and AHA grant 14GRNT18730054 (to MFN), NIH grant T32HL086350 (to AUS and MAN), AHA 16SDG27260070 (to MAN), NIH grant R01DK057236 (to SMW), NIH grant R01HL085870 (to LFS), NIH grants R01MH097887, R01AG055357 and R01NS078792 (to JWH) and a UC Davis Academic Federation Innovative Development Award (to MN-C).

## Author Contributions

M.N.-C. and M.F.N. conceived, designed, and executed experiments; collected, analyzed and interpreted data; and wrote and revised the manuscript. A.U.S., O.R.B., R.R.R., M.A.N. and D.G. executed experiments, collected, and analyzed data, and revised the manuscript. K.C.S. and S.M.W. contributed human samples critical to this work, information about patients, and revised the manuscript. L.F.S. and J.W.H. designed experiments, interpreted results and revised the manuscript.

## Additional Information

**Supplementary information** accompanies this paper at <https://doi.org/10.1038/s41598-017-14565-9>.

**Competing Interests:** The authors declare that they have no competing interests.

**Publisher's note:** Springer Nature remains neutral with regard to jurisdictional claims in published maps and institutional affiliations.



**Open Access** This article is licensed under a Creative Commons Attribution 4.0 International License, which permits use, sharing, adaptation, distribution and reproduction in any medium or format, as long as you give appropriate credit to the original author(s) and the source, provide a link to the Creative Commons license, and indicate if changes were made. The images or other third party material in this article are included in the article's Creative Commons license, unless indicated otherwise in a credit line to the material. If material is not included in the article's Creative Commons license and your intended use is not permitted by statutory regulation or exceeds the permitted use, you will need to obtain permission directly from the copyright holder. To view a copy of this license, visit <http://creativecommons.org/licenses/by/4.0/>.

© The Author(s) 2017